

## Two-Step Fluorescence Screening of CD21-Binding Peptides with One-Bead One-Compound Library and Investigation of Binding Properties of *N*-(2-Hydroxypropyl)methacrylamide Copolymer–Peptide Conjugates

Hui Ding,<sup>†</sup> Wolfgang M. Prodinge,<sup>§</sup> and Jindřich Kopeček<sup>\*,†,‡</sup>

Departments of Pharmaceutics and Pharmaceutical Chemistry, and Bioengineering, University of Utah, Salt Lake City, Utah 84112, and Department of Hygiene, Microbiology and Social Medicine, Innsbruck Medical University, Innsbruck, Austria

Received May 24, 2006; Revised Manuscript Received August 6, 2006

Using the one-bead one-compound (OBOC) combinatorial method, four heptapeptide ligands of CD21 receptor, a cell surface marker of malignant B cell lymphoma, were identified with an innovative two-step fluorescence screening method to overcome the limitation caused by autofluorescence of TentaGel resin. The binding affinities of selected peptides, YILHRN (**B1**), PTLDDL (**B2**), and LVLLTRE (**B3**), were in the micromolar region as determined by a fluorescence quenching assay. Peptide **B1** was conjugated to *N*-(2-hydroxypropyl)methacrylamide (HPMA) copolymer via spacers of different lengths, composed of one to four repeats of the 8-amino-3,6-dioxaoctanoic acid (A) group. The evaluation of the biorecognizability of HPMA copolymer–**B1** conjugates by the CD21 receptor revealed that increasing the number of repeats of A in the spacer from one to three resulted in continuous improvements in the biorecognition by the CD21 receptor; the increase from three to four repeats showed no significant effect. This work showed the potential of the OBOC combinatorial approach to select peptide ligands as targeting moieties for CD21 specific polymeric drug carriers.

### Introduction

The water-soluble *N*-(2-hydroxypropyl)methacrylamide (HPMA) copolymer is an extensively studied anticancer drug carrier.<sup>1,2</sup> As other water-soluble macromolecules,<sup>1,3</sup> HPMA copolymer–drug conjugates accumulate passively in solid tumors as a result of enhanced permeation and retention (EPR) effect.<sup>4,5</sup> Active targeting of HPMA copolymer–drug conjugates can be achieved with the incorporation of cancer cell specific ligands, such as carbohydrates,<sup>6</sup> lectins,<sup>7</sup> antibodies,<sup>8,9</sup> antibody fragments,<sup>10,11</sup> and peptides,<sup>12,13</sup> resulting in enhanced uptake of conjugates by cancer cells through receptor-mediated endocytosis with concomitant improvement of therapeutic efficacy. Among different cancer targeting molecules, peptides are of particular interest, as they may be readily identified with combinatorial peptide libraries.<sup>14</sup> Enhanced peptide targeting efficiency could be achieved through multivalent interactions between targets and HPMA copolymer–peptide conjugates containing multiple copies of peptides within a single polymer chain.<sup>12,15</sup>

Antigenic targets of lymphoma include receptors CD19, CD20, CD22, and CD37.<sup>16</sup> The CD21 receptor (complement receptor 2, CR2) is expressed primarily on mature B lymphocytes, and also on epithelial cells, thymocytes, and follicular dendritic cells.<sup>17</sup> Overexpression of CD21 receptor was found on lymphoblastoid cell lines such as Raji cells;<sup>18</sup> consequently, it has been used as an alternative target for lymphomas.<sup>12,19</sup> CD21 receptor is a 145 kDa transmembrane glycoprotein with

its extracellular region consisting of 15–16 short consensus repeats (SCRs), of which SCR1 and SCR2 are responsible for the interaction with several natural ligands, such as C3d, C3dg, and Epstein Barr virus (EBV).<sup>17</sup> Gold particles coated with C3dg were internalized into Raji cells (CD21 positive) through a receptor-mediated endocytosis by CD21 receptor.<sup>20</sup> Therefore, CD21 targeting could not only direct the tumor specific delivery of anticancer drugs, but also mediate their internalization, thus providing a suitable target for a HPMA copolymer-based delivery system for lymphoma chemotherapy. For convenience, a truncated recombinant CD21 receptor, rsCR2.1–4,<sup>21</sup> was prepared. rsCR2.1–4 consists of the first four SCRs of CD21 receptor, and it is fully functional in interactions with ligands of CD21 receptor. Therefore, it was used as a target molecule for the screening of peptide ligands of CD21 receptor with combinatorial peptide libraries in this work.

The emergence of combinatorial peptide library techniques has dramatically expedited the screening and identification of novel peptides with desired properties.<sup>22</sup> The methods to prepare combinatorial peptide libraries can be generally divided into two categories: chemically prepared libraries, using methods such as one-bead one-compound (OBOC)<sup>23–25</sup> and SPOT synthesis;<sup>26,27</sup> and biologically prepared libraries, using methods such as phage display<sup>28,29</sup> and bacterial display.<sup>30,31</sup> Both OBOC and phage display methods have been extensively used for selection and identification of oligopeptide ligands for tumor targeting.<sup>14</sup> However, most of the peptide ligand identification studies ended at verifying the validity of identified sequences, without evaluating their potentials in drug delivery systems applications.

Previously, five distinctive pentadecapeptide ligands of CD21 receptor were identified with phage display, and the specificity of selected peptides was confirmed by phage enzyme-linked immunosorbent assay (ELISA) and competitive phage ELISA.<sup>15</sup>

\* To whom correspondence should be addressed. Phone: (801) 581-7211. Fax: (801) 581-7848. E-mail: jindrich.kopecek@utah.edu.

<sup>†</sup> Department of Pharmaceutics and Pharmaceutical Chemistry, University of Utah.

<sup>‡</sup> Department of Bioengineering, University of Utah.

<sup>§</sup> Innsbruck Medical University.

The dissociation constants of three peptides, RMWPSSTVNL-SAGRR (**P1**), PNLDFSPTCSFRFGC (**P2**), and GRVPSMFG-GHFFFSR (**P3**), were determined to be within the micromolar range with a fluorescence quenching assay. To verify the applicability of selected peptides for targeting within a polymeric drug delivery system, the binding properties of HPMA copolymer–**P1** conjugate were examined with surface bound CD21 receptor. It was found that peptide **P1** retained its biorecognizability after it was conjugated with HPMA copolymer and that the multivalency effect was important for interaction between the conjugate and the receptor.<sup>15</sup> Interestingly, varying the length of spacer between peptide **P1** and polymer backbone had a trivial effect on the conjugate binding, suggesting that peptide **P1** was readily accessible for interaction.

Alternatively, peptide ligands of CD21 receptor could also be identified using the one-bead one-compound (OBOC) method with a two-step fluorescence screening process. On the basis of the “split and mix” concept,<sup>32,33</sup> Lam et al. developed an OBOC combinatorial method, which consists of library preparation, biological screening, and structure determination of individual hits.<sup>23</sup> With OBOC, a peptide library containing millions of different peptides can be synthesized on a resin so that each bead contains only one distinctive peptide. A most widely used solid support is the TentaGel resin, which has good swelling properties in both organic solvent and aqueous solutions.<sup>24</sup> However, fluorescence screening, one of the most direct and convenient screening methods, of peptide libraries on TentaGel resin has been greatly limited, because of the autofluorescence of the TentaGel resin.<sup>34,35</sup>

In this work, four heptapeptide ligands of CD21 receptor, YILHRN (**B1**), PTLDLPL (**B2**), LVLLTRE (**B3**), and IV-FLLVQ (**B4**), were identified with the OBOC method using a two-step fluorescence screening method to avoid the limitation caused by autofluorescence of TentaGel. The binding affinities of selected heptapeptides, except the hydrophobic **B4**, were determined with a fluorescence quenching assay. Peptide **B1** was conjugated to *N*-(2-hydroxypropyl)methacrylamide (HPMA) copolymer via spacers of different length, composed of one to four repeats of the 8-amino-3,6-dioxaoctanoic acid (A) group (Figure 1). The biorecognizability of these HPMA copolymer–**B1** conjugates by the CD21 receptor was evaluated. Finally, the results on the biorecognition of HPMA copolymer conjugates, containing either a heptapeptide selected by OBOC or a pentadecapeptide selected by phage display, were compared.

## Experimental Procedures

**Materials.** Soluble CD21 receptor (SCD21)<sup>19</sup> and rsCR2.1–4<sup>21</sup> were prepared as previously described. TentaGel S NH<sub>2</sub> was purchased from Peptides International, Inc. 2-Chlorotriethyl chloride resin, MBHA (4-methylbenzhydrylamine) resin, and all *N*- $\alpha$ -Fmoc protected amino acids were purchased from Novabiochem.

**Synthesis of the One-Bead One-Compound Peptide Library.** TentaGel S NH<sub>2</sub> (2 g; 90  $\mu$ m, 0.24 mmol/g substitution) was used as the solid support for the synthesis of a heptapeptide library. The library was synthesized with standard solid-phase 9-fluorenylmethoxycarbonyl (Fmoc) chemistry using the “split and mix” method. TentaGel S NH<sub>2</sub> was first swollen to equilibrium in DMF overnight and then evenly distributed into 19 vials. Different *N*- $\alpha$ -Fmoc protected amino acids (19 natural amino acids excluding cysteine) were loaded onto the resin in the presence of DIC/HOBt. The completeness of reaction was monitored with bromophenol blue. After the first amino acid was loaded, all of the resin was mixed together and washed with DMF. The Fmoc protection was removed by incubation twice with 25% piperidine/DMF, and the resin was washed with DMF. The resin was

again distributed evenly into 19 vials, and coupling of the remaining amino acids was repeated as described above. The side-chain protection was removed by incubation with phenol/thioanisole/H<sub>2</sub>O/EDT/trifluoroacetic acid (TFA) (0.75:0.5:0.5:0.25:10, w/v/v/v/v) at room temperature for 2.5 h. Finally, the resin was washed serially with DMF, methanol, DCM, DMF, 30% H<sub>2</sub>O/DMF, 60% H<sub>2</sub>O/DMF, 100% H<sub>2</sub>O, and phosphate-buffered saline (PBS). The resin was stored in 0.05% sodium azide/PBS at 4 °C.

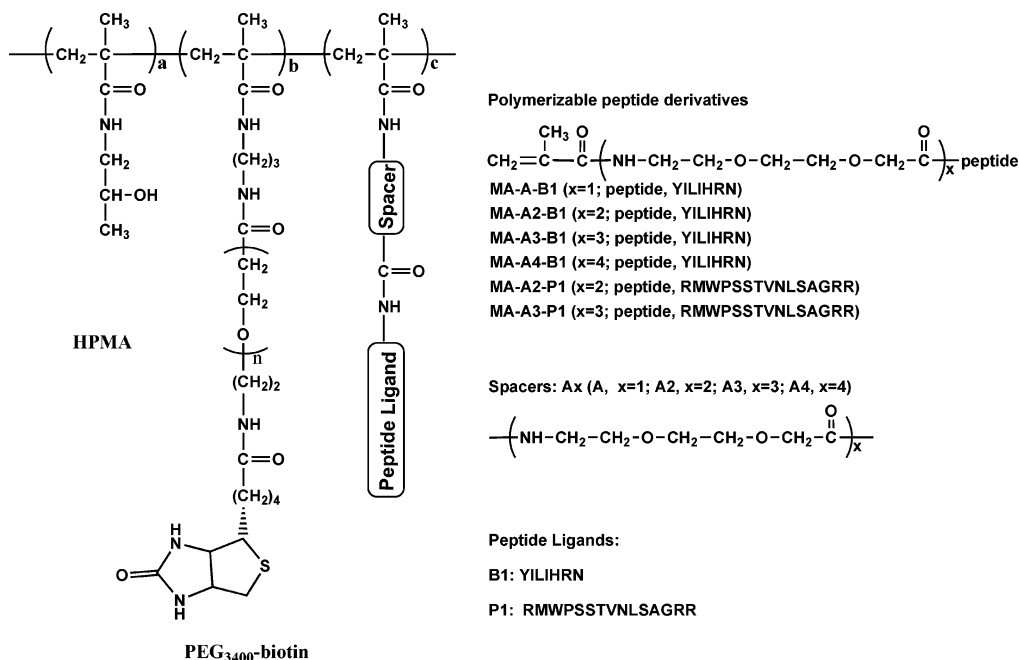
**Fluorescent Labeling of rsCR2.1–4.** rsCR2.1–4 was labeled with two different F/P (number of fluorophores per protein) ratios, 1 and 5. To a solution of rsCR2.1–4 in 200  $\mu$ L of PBS (0.5 mg/mL), 20  $\mu$ L of 1 M NaHCO<sub>3</sub> (pH 9.0) and 23.3  $\mu$ L of FITC in dimethyl sulfoxide (DMSO) (10 mg/mL) were added, and the reaction was stirred for 1 h (F/P  $\approx$  1) or 5 h (F/P  $\approx$  5) at room temperature in the dark. To remove free FITC, the reaction mixture was diluted to 0.5 mL with PBS and immediately applied to a PD-10 column (Amersham Biosciences) pre-equilibrated with PBS buffer. The concentration of the fluorescently labeled protein and labeling efficiency were determined using UV spectrometry.

**Two-Step Fluorescence Screening of Peptide Ligands of CD21 Receptor with FITC-Labeled rsCR2.1–4.** *First Step: Screening of Fluorescence Positive Beads with Bound Receptor.* TentaGel beads containing the peptide library (2 mL; approximately  $1 \times 10^6$  beads) were transferred to a polypropylene column. After being washed with water, the beads were blocked with 0.1% gelatin in water, followed by washing with 0.1% PBS containing 0.1% Tween 20 (TPBS). Next, the beads were incubated with FITC-labeled rsCR2.1–4 (F/P  $\approx$  1, 0.02  $\mu$ M) for 1 h with gentle shaking. The unbound receptor was washed off with TPBS. The beads were then transferred to several Petri dishes, and fluorescently bright beads were picked under a fluorescence microscope (Nikon ECLIPSE E800); a total of 48 beads were selected.

*Second Step: Screening of Fluorescence Negative Beads after Treating with Guanidium Hydrochloride (Gu·HCl).* Selected beads were divided into two groups on the basis of their physical appearance: opaque fluorescence (27 beads) and transparent fluorescence (21 beads). Both groups of beads were treated with Gu·HCl (6 M, pH 1.0) for 3 h. Because Gu·HCl can disrupt the binding of receptor to corresponding peptide ligands, it was used to differentiate the autofluorescence of TentaGel beads. It was found that beads with initial opaque fluorescence lost the fluorescence after treatment with Gu·HCl; however, the fluorescence of beads with initial transparent fluorescence was retained, an indication of autofluorescence. The fluorescence of opaque fluorescence beads was recovered after washing the beads with PBS and incubation with FITC labeled rsCR2.1–4, but with lower intensity.

**Synthesis of Peptides.** Peptides, YILHRN (**B1**), PTLDLPL (**B2**), and LVLLTRE (**B3**), were synthesized manually on a solid support of 2-chlorotriethyl chloride resin using standard Fmoc chemistry. The synthesized peptides were cleaved from resin with a mixture of TFA: H<sub>2</sub>O:triisopropylsilane (TIS) (95:2.5:2.5, v/v/v) for 4 h at room temperature. All synthesized peptides were purified with RP-HPLC and verified with matrix-assisted laser desorption/ionization time-of-flight mass spectrometry (MALDI-TOF MS). MALDI-TOF MS calculated for **B1** (MH<sup>+</sup>) 928.53, found 928.61; MALDI-TOF MS calculated for **B2** (MH<sup>+</sup>) 752.41, found 752.42; MALDI-TOF MS calculated for **B3** (MH<sup>+</sup>) 843.52, found 843.72.

**Determination of Peptide Binding Constants with Fluorescence Quenching.** A series of mixtures of the labeled receptor rsCR2–FITC at 0.02  $\mu$ M and peptides, **B1**, **B2**, and **B3**, at different concentrations were prepared in 150  $\mu$ L of PBS. The mixtures were incubated at room temperature for 5 h. The fluorescence intensity of each sample was measured in duplicates with a LS-55 luminescence spectrometer (Perkin-Elmer) with excitation and emission wavelengths of 495 and 515 nm, respectively. The fluorescence background caused by the peptides was negligible within the concentration range used. The association constant was estimated by fitting the quenching data to eq



Polymer Conjugates	Spacer	Spacer Structure	Peptide
P <sup>B</sup>	N/A	N/A	N/A
P <sup>B</sup> -A-B1	A	-NH-(CH <sub>2</sub> ) <sub>2</sub> -O-(CH <sub>2</sub> ) <sub>2</sub> -CH <sub>2</sub> -CO-	YILHRN
P <sup>B</sup> -A2-B1	A2	-[NH-(CH <sub>2</sub> ) <sub>2</sub> -O-(CH <sub>2</sub> ) <sub>2</sub> -CH <sub>2</sub> -CO] <sub>2</sub> -	YILHRN
P <sup>B</sup> -A3-B1	A3	-[NH-(CH <sub>2</sub> ) <sub>2</sub> -O-(CH <sub>2</sub> ) <sub>2</sub> -CH <sub>2</sub> -CO] <sub>3</sub> -	YILHRN
P <sup>B</sup> -A4-B1	A4	-[NH-(CH <sub>2</sub> ) <sub>2</sub> -O-(CH <sub>2</sub> ) <sub>2</sub> -CH <sub>2</sub> -CO] <sub>4</sub> -	YILHRN
P <sup>B</sup> -A2-P1	A2	-[NH-(CH <sub>2</sub> ) <sub>2</sub> -O-(CH <sub>2</sub> ) <sub>2</sub> -CH <sub>2</sub> -CO] <sub>2</sub> -	RMWPSSTVNLSAGRR
P <sup>B</sup> -A3-P1	A3	-[NH-(CH <sub>2</sub> ) <sub>2</sub> -O-(CH <sub>2</sub> ) <sub>2</sub> -CH <sub>2</sub> -CO] <sub>3</sub> -	RMWPSSTVNLSAGRR

**Figure 1.** Structures of polymerizable peptide derivatives and HPMA copolymer-peptide conjugates. P<sup>B</sup>, HPMA copolymer backbone labeled with a PEG<sub>3400</sub>-biotin graft; HPMA copolymer-peptide conjugates consist of three components, an HPMA copolymer backbone, a PEG-biotin graft used as a label for immunoassay, and peptide ligands with spacers of different lengths, A1, A2, A3, and A4. P<sup>B</sup>-A-B1, P<sup>B</sup>-A2-B1, P<sup>B</sup>-A3-B1, and P<sup>B</sup>-A4-B1, peptide B1 attached to the HPMA copolymer backbone via spacers A, A2, A3, and A4. P<sup>B</sup>-A2-P1 and P<sup>B</sup>-A3-P1, peptide P1 attached to the HPMA copolymer backbone via spacers A2 and A3.

1 with the software KaleidaGraph (version 3.0).<sup>36</sup>

$$Q = \frac{Q_m K_a [P]}{1 + K_a [P]} \quad (1)$$

$$Q = \frac{F_0 - F}{F} \quad (2)$$

where  $Q$  is the quenching value defined in eq 2,  $Q_m$  represents maximal fluorescence quenching,  $K_a$  is the association constant of peptide binding, and  $[P]$  is the concentration of free peptide.  $F_0$  and  $F$  are fluorescence intensities of fluorescently labeled rsCR2.1-4 in the absence and presence of peptide ligands, respectively.

**Synthesis of Polymerizable Peptide Derivatives.** Polymerizable *N*-methacryloylated peptides containing spacers of repeating units of 8-amino-3,6-dioxaoctanoic acid (A), methacryloyl (MA)-A-B1, MA-A2-B1, MA-A3-B1, MA-A4-B1, MA-A2-P1, and MA-A3-P1 (P1, RMWPSSTVNLSAGRR, was selected by phage display<sup>15</sup>), were synthesized (see structures in Figure 1) on MBHA resin using standard Fmoc chemistry. After the peptides were synthesized on resin,

they were extended with additional spacers; A, 8-amino-3,6-dioxaoctanoyl-8-amino-3,6-dioxaoctanoic acid (A2), 8-amino-3,6-dioxaoctanoyl-8-amino-3,6-dioxaoctanoic acid (A3), and 8-amino-3,6-dioxaoctanoyl-8-amino-3,6-dioxaoctanoic acid (A4) spacers were added by coupling with one, two, three, or four repeats of Fmoc-A (9-fluorenylmethoxycarbonyl-8-amino-3,6-dioxaoctanoic acid, Peptides International) and capped with methacryloyl chloride. All peptide monomers were purified with RP-HPLC and were verified with MALDI-TOF MS. MALDI-TOF MS calculated for MA-A-B1 (MH<sup>+</sup>) 1140.65, found 1140.70; MALDI-TOF MS calculated for MA-A2-B1 (MH<sup>+</sup>) 1285.72, found 1285.79; MALDI-TOF MS calculated for MA-A3-B1 (MH<sup>+</sup>) 1430.79, found 1430.82; MALDI-TOF MS calculated for MA-A4-B1 (MH<sup>+</sup>) 1575.87, found 1575.87; MALDI-TOF MS calculated for MA-A2-P1 (MH<sup>+</sup>) 2076.06, found 2076.11; MALDI-TOF MS calculated for MA-A3-P1 (MH<sup>+</sup>) 2220.13, found 2220.25.

**Synthesis of MA-PEG<sub>3400</sub>-Biotin.** MA-PEG<sub>3400</sub>-biotin was synthesized as described previously.<sup>15</sup> Briefly, *N*-(3-aminopropyl)-methacrylamide hydrochloride (MA-NH<sub>2</sub>) (2.7 mg) was dissolved in



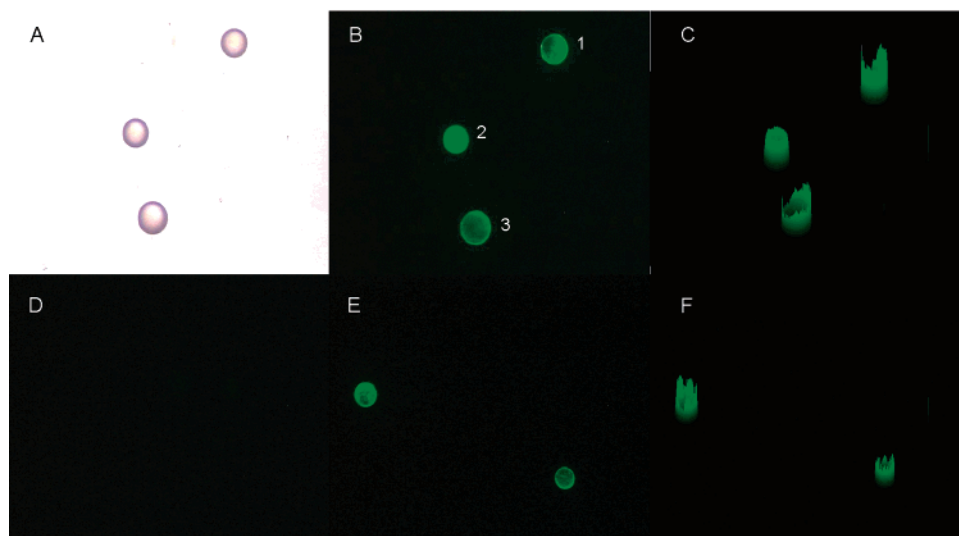


**Figure 2.** Two-step fluorescence screening of OBOC peptide library: (A) DIC image of TentaGel beads; (B) fluorescence positive beads; beads 1 and 3 are fluorescence transparent; bead 2 is fluorescence opaque; (C) surface plot of fluorescence of beads in (B); (D) the fluorescence of fluorescence opaque beads disappeared after treatment with Gu·HCl; (E) the fluorescence of fluorescence transparent beads remained after treatment with Gu·HCl; and (F) surface plot of fluorescence of beads in (E).

200  $\mu\text{L}$  of DMF, and 6.7  $\mu\text{L}$  of *N,N*-diisopropylethylamine (DIPEA) was added. The temperature of the solution was lowered to 0  $^{\circ}\text{C}$  with an ice bath. Biotin-PEG<sub>3400</sub>-*N*-hydroxysuccinimide ester (NHS) (PEG, poly(ethylene glycol), mol. wt. 3400; NHS, *N*-hydroxysuccinimide ester; Nektar Therapeutics) dissolved in 200  $\mu\text{L}$  of DMF was added dropwise. The reaction was kept at 0  $^{\circ}\text{C}$  for 30 min and then left overnight at room temperature. The crude product was diluted 1:1 with water and MA-PEG<sub>3400</sub>-biotin purified on a PD-10 column. Molecular weight as determined by MALDI-TOF MS was  $M_w = 3.89$  kDa;  $M_n = 3.86$  kDa;  $M_w/M_n = 1.01$ .

**Synthesis of Biotin-Labeled HPMA Copolymer–Peptide Conjugates (See Structures in Figure 1).** The synthesis of HPMA copolymer–peptide conjugate P<sup>B</sup>–GG–B1 (P<sup>B</sup> is HPMA copolymer backbone labeled with a PEG<sub>3400</sub>–biotin graft) is described as an example: HPMA (14.1 mg), MA–A–B1 (6 mg), MA-PEG<sub>3400</sub>–biotin (3.6 mg) (molar ratio, 94:5:1), and initiator 2,2'-azobisisobutyronitrile (AIBN) (1.5 mg) were dissolved in 149  $\mu\text{L}$  of DMSO in a glass ampule. The solution was bubbled with nitrogen for 10 min and polymerized in the sealed ampule at 50  $^{\circ}\text{C}$  for 24 h. After the reaction was finished, the reaction solution was diluted to 3 mL with H<sub>2</sub>O and dialyzed against water in dialysis tubing with a molecular cutoff of 12–14 kDa for 3 days. After dialysis, the polymer water solution was lyophilized. P<sup>B</sup>, P<sup>B</sup>–A2–B2, P<sup>B</sup>–A3–B3, P<sup>B</sup>–A4–B1, P<sup>B</sup>–A2–P1, and P<sup>B</sup>–A3–P1 were synthesized similarly, except that P<sup>B</sup> contained no peptide. The polymers were analyzed with size-exclusion chromatography on an ÄKTA FPLC system (Pharmacia). The content of peptide was determined by amino acid analysis, and the content of biotin was determined with the EZ Biotin Quantitation Kit (PIERCE Biotech, Inc.).

**ELISA of HPMA Copolymer–Peptide Conjugates.** The receptor rsCR2.1–4 (150 ng) was coated onto a MaxiSorp plate by overnight incubation at 4  $^{\circ}\text{C}$ . The plate was blocked with 4% milk at room temperature for 1.5 h, washed with TPBS, and incubated with HPMA copolymer–peptide conjugates (0.02  $\mu\text{M}$ ) for 30 min. Next, the plate was washed five times with TPBS, followed by incubation with streptavidin/horseradish peroxidase (HRP) (Zymed Laboratories) for 30 min. The plate was washed five times with TPBS, and then 3,3',5,5'-tetramethylbenzidine (TMB) substrate was added to the plate and incubated for 30 min. The absorbance was read at 450/630 nm.

## Results

**Synthesis of the One-Bead One-Compound Peptide Library.** A heptapeptide library containing more than one million

different peptides was synthesized with the one-bead one-compound method. TentaGel S NH<sub>2</sub> resin was used as solid support, and peptides were synthesized with manual solid-phase Fmoc peptide synthesis. It was noted that the coupling reactions of hydrophobic and bulky residues proceeded slower than those of small and hydrophilic residues. However, almost all of the reactions were able to finish within 1 h as indicated by analysis with bromophenol blue. To ensure the quality of synthesized library, a control heptapeptide with a known sequence, HPLSSSV, was synthesized along with the heptapeptide library. The composition of control peptide was confirmed by automated Edman sequencing. Therefore, the purity of the synthesized heptapeptide library should be usable for the following biological screening.

**Two-Step Fluorescence Screening of Peptide Ligands for CD21 Receptor.** To minimize the influence of FITC labeling on the receptor binding, rsCR2.1–4 with a low fluorescence label content (F/P  $\approx$  1) was used for screening peptide ligands of CD21 receptor. By fluorescently labeling the recombinant short CD21 receptor, rsCR2.1–4, the binding of receptor to its peptide ligands can be conveniently identified with fluorescence visualization. However, we found, in agreement with previous reports, that a very small number of TentaGel beads are autofluorescent,<sup>34,35</sup> which largely limited the fluorescence screening process. In this work, an innovative two-step fluorescence screening process was developed: in the first step, 48 most fluorescently bright beads were picked; in the second step, 27 fluorescence negative beads were picked after all of the beads from the first step were treated with Gu·HCl (6 M, pH 1). Gu·HCl is a strong protein chaotropic agent, and it disrupts the binding between rsCR2.1–4 and bead-bound peptides, resulting in the disappearance of fluorescence. However, the fluorescence of the beads, which possessed autofluorescence, was not susceptible to Gu·HCl, and the fluorescence did not change after treatment with Gu·HCl. Therefore, fluorescence negative beads in the second step actually contained real peptide ligands of the receptor.

In fact, fluorescence of the selected beads in the first screening step showed two different appearances: opaque and transparent (Figure 2). Beads with opaque fluorescence seemed to have homogeneous fluorescence as well; on the contrary, beads with

**Table 1.** Peptide Ligands of CD21 Receptor Identified with OBOC

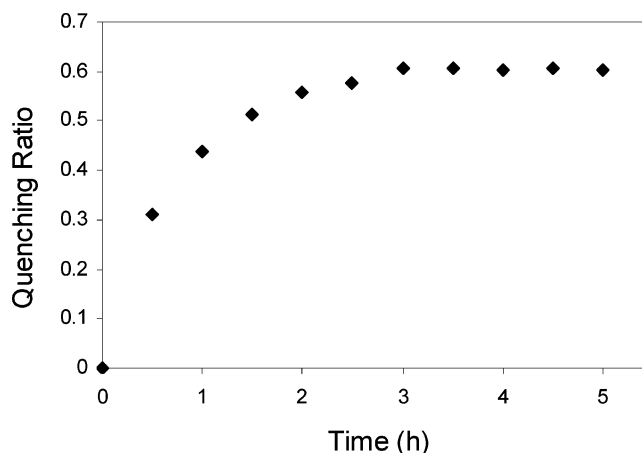
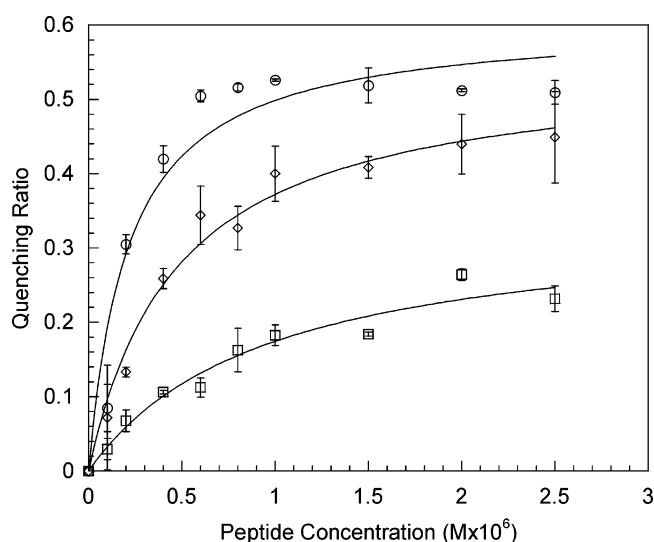
peptide	sequence	binding constant, $K_a$ ( $M^{-1}$ )
B1	YILIHNR	$4.6 \times 10^6$
B2	PTLDPLP	$1.0 \times 10^6$
B3	LVLLTRE	$2.1 \times 10^6$
B4	IVFLLVQ	ND <sup>a</sup>

<sup>a</sup> ND: not determined.

transparent fluorescence seemed to have heterogeneous fluorescence. All beads selected in the first step were divided into two groups on the basis of their fluorescence appearance: one group with opaque fluorescence and the other with transparent appearance. After both groups were treated with  $Gu \cdot HCl$ , the fluorescence of all beads in the opaque group disappeared, while the fluorescence of the transparent group remained. Furthermore, the spatial fluorescence distribution of selected beads was characterized with surface plotting using the software of Image Pro Plus version 4.0 (Figure 2C and F). It was found that spatial fluorescence distribution of fluorescence opaque beads and transparent beads was clearly different. The fluorescence distribution of transparent beads was heterogeneous with rugged surfaces, while that of opaque fluorescence beads was homogeneous with smooth surfaces. Therefore, it was deduced that fluorescence of transparent beads with heterogeneous distribution is probably the result of autofluorescence. Although there is not enough evidence to prove it, this fact may be used as a cross-reference in fluorescence screening process.

With the two-step screening process, we were able to select 27 beads that matched our criteria. Those beads were washed with TPBS and allowed to incubate with FITC labeled rsCR2.1–4 again. The regaining of fluorescence confirmed their binding to CD21 receptor, however, with diminished intensity. Probably, the binding has been significantly weakened by the prior treatment with  $Gu \cdot HCl$ . Finally, we selected the four most fluorescently bright beads and analyzed the peptide sequences by Edman sequencing (Table 1). It was found that peptides **B1** (YILIHNR), **B3** (LVLLTRE), and **B4** (IVFLLVQ) have similar structures: the first four amino acids at the N-terminus were composed of hydrophobic residues, mostly of leucine, isoleucine, and valine. One may speculate that these hydrophobic residues mediate hydrophobic interactions with the CD21 receptor.

**Binding Constant Determination with Fluorescence Quenching.** It was found that fluorescence quenching due to the binding of peptides was not apparent when the labeling of rsCR2.1–4 was low ( $F/P \approx 1$ ) (data not shown). When the labeling of rsCR2.1–4 was high ( $F/P \approx 5$ ), the quenching effect was sufficient for the determination of binding affinity. On the basis of X-ray crystallography of free CD21 (SCR1-2) and the complex of CD21 (SCR1-2) and C3d,<sup>37,38</sup> it was found that two domains of SCR1 and SCR2 formed a V-shaped structure and these two domains were glued together through extensive side-by-side hydrophobic interactions. The binding of C3d to CD21 receptor induced not only local but also global conformational changes, which suggested that the CD21 receptor (or at least SCR1-2) is a relatively flexible molecule and the binding of CD21 receptor to its ligands was an induced-fitting process.<sup>37</sup> This induced-fitting process may change the microenvironment of fluorophore of FITC-labeled rsCR2.1–4, resulting in change of fluorescence intensity, therefore providing a convenient way for measuring the binding affinity of the peptide–receptor interaction. Meanwhile, this induced-fitting process may also influence the time required to reach binding equilibrium. As

**Figure 3.** Binding kinetics of peptide YILIHNR to rsCR2.1–4. YILIHNR ( $3 \mu M$ ) was incubated with rsCR2.1–4 ( $0.02 \mu M$ ), and the fluorescence quenching ratio was determined as a function of time.**Figure 4.** Fluorescence quenching of fluorescein-labeled rsCR2.1–4 as a function of peptide concentration. Data are depicted as mean  $\pm$  standard deviation from duplicate measurements. ( $\circ$ ) peptide **B1**, YILIHNR; ( $\square$ ) peptide **B2**, PTLDPLP; ( $\diamond$ ) peptide **B3**, LVLLTRE.

indicated in our binding kinetics study of peptide YILIHNR, it took about 3 h to reach quenching equilibrium, although more than one-half of maximal quenching was achieved within the first half an hour (Figure 3). Consequently, in binding constant determination studies, fluorescence intensity was measured after the peptides and receptor were incubated for 5 h.

The binding affinity of **B4** (IVFLLVQ) was not determined, because of its excessive hydrophobicity as implied by its sequence composition. The association constants of peptides **B1**, **B2**, and **B3** were determined to be  $4.6 \times 10^6 M^{-1}$  (fitting error = 1.4;  $R = 0.97$ ),  $1.0 \times 10^6 M^{-1}$  (fitting error = 0.3;  $R = 0.98$ ), and  $2.1 \times 10^6 M^{-1}$  (fitting error = 0.3;  $R = 0.99$ ), respectively (Figure 4).

**Synthesis and Characterization of HPMA Copolymer–Peptide Conjugates.** All HPMA copolymer conjugates were synthesized by radical copolymerization of HPMA with polymerizable derivatives of peptide and biotin using 2,2'-azobisisobutyronitrile (AIBN) as the initiator. The composition of the synthesized polymers is summarized in Table 3. The weight-average molecular weight was determined with size-exclusion chromatography on a Sepharose 6B column calibrated with polyHPMA (PHPMA) standards. Copolymerization with a small amount of MA–PEG<sub>3400</sub>–biotin provided a convenient way to

**Table 2.** Comparison of Peptide Sequences Obtained from Phage Display and OBOC

phage display <sup>15</sup>	OBOC (this work)
RMWPSSTVNLSAGRR	
<b>PNLDFSPTCSFRFGC<sup>a</sup></b>	<b>PTLDPLP<sup>a</sup></b>
GRVPSMFGGHFFSR	
RLAYWCFSG <b>LFLLC<sup>a</sup></b>	<b>LVLLTRE, IVLLVQ, YILHNR<sup>a</sup></b>
PVAASVFPYLVKTY	

<sup>a</sup> The similar residues of peptides selected from phage display and OBOC are indicated by boldface italic type.

monitor the interaction between HPMA copolymer-peptide conjugates and CD21 receptor using the biotin/streptavidin-HRP detection system in ELISA experiments. Only 1 mol % of MA-PEG<sub>3400</sub>-biotin was used in the monomer feed, and the polymer conjugates contained approximately one biotin per macromolecule (Table 3).

**Effect of Spacer Length on Binding of HPMA Copolymer-Peptide Conjugates to CD21 Receptor.** The binding of HPMA copolymer-peptide conjugates with surface bound receptor was detected with ELISA using biotin/streptavidin/HRP as the reporting system. Nonspecific binding was blocked with 4% nonfat milk as it was found to produce the lowest background. Although milk contains various amounts of endogenous biotin, which may interfere with the biotin/streptavidin/HRP detection system, it did not seem to cause any problems in the binding studies in this work. If the endogenous biotin were to interact with the detection system, it can be masked with egg white and milk.<sup>39</sup>

Peptide **B1** was used as an example to study the binding properties of HPMA copolymer-peptide conjugates as **B1** demonstrated the best binding affinity with good solubility. To evaluate whether spacer length has a significant effect on the binding of HPMA copolymer-**B1** conjugates to CD21 receptor, a series of conjugates, P<sup>B</sup>-A-**B1**, P<sup>B</sup>-A2-**B1**, P<sup>B</sup>-A3-**B1**, and P<sup>B</sup>-A4-**B1** (Figure 1), were prepared, which differed in spacer length. Because of its flexibility and moderate hydrophilicity, 8-amino-3,6-dioxaoctanoic acid (A) was used as repeating units of spacers, A, A2 (dimer of A), A3 (trimer of A), and A4 (tetramer of A), between peptide and polymer backbone. The binding results of these four peptide conjugates with different spacers (**B1** concentration 0.02  $\mu$ M) are shown in Figure 5. All conjugates showed better binding to the surface with receptor than to the surface without receptor. Most importantly, a clear spacer effect on the surface binding was observed. The conjugate with the shortest spacer, P<sup>B</sup>-A-**B1**, showed the weakest binding. With the increase of spacer length (from A to A3), the binding increased significantly. This spacer effect on the binding may be ascribed to the decreased accessibility of a peptide after its conjugation with a polymer,<sup>40</sup> but the accessibility of the peptide can be improved by using the proper spacer. A further increase in spacer length, from A3 to A4, did not result in an improvement of binding. It appears that spacer A3 was sufficient for presenting the targeting peptide **B1**; the peptide is fully accessible with either spacer A3 or A4.

**ELISA of HPMA Copolymer-B1 Conjugate Binding to Surfaces with Different Amounts of rsCR2.1-4.** P<sup>B</sup>-A3-**B1** was used to study its specific interaction with surface bound receptor, rsCR2.1-4. MaxiSorp plate was coated with different amounts of rsCR2.1-4 (0-240 ng), which resulted in varied density of surface bound receptor. The binding of a fixed amount of P<sup>B</sup>-A3-**B1** (0.02  $\mu$ M) was detected with ELISA using biotin/streptavidin-HRP as the reporting system. The binding of P<sup>B</sup>-A3-**B1** to surface bound receptor was directly related to the receptor density: the higher was the receptor density,

the higher was the amount of surface bound P<sup>B</sup>-A3-**B1** (Figure 6). When the MaxiSorp plate surface was coated with 7.5 ng of rsCR2.1-4, the binding of P<sup>B</sup>-A3-**B1** was comparable to that of the control surface containing no receptor; when surface was coated with a double amount of rsCR2.1-4 (15 ng), the binding signal increased almost 10 times. However, subsequent doubling of the coated amount of rsCR2.1-4 only increased the binding signal less than twice. This direct response of P<sup>B</sup>-A3-**B1** binding to surface bound receptor density corroborated the specific interaction between HPMA copolymer-peptide conjugate and receptor. High receptor density was favorable for the multivalent interaction between P<sup>B</sup>-A3-**B1** and surface bound receptor.

**Comparison of Surface Binding of HPMA Copolymers Containing Peptides B1 and P1.** The binding properties of HPMA copolymer-**P1** conjugates were studied previously.<sup>15</sup> Here, their surface binding was compared to that of HPMA copolymer-**B1** conjugates. Four HPMA copolymer-peptide conjugates, P<sup>B</sup>-A2-**B1**, P<sup>B</sup>-A3-**B1**, P<sup>B</sup>-A2-**P1**, and P<sup>B</sup>-A3-**P1**, were incubated with three different surfaces: control surface without any receptor, surface coated with rsCR2.1-4, and surface coated with sCD21,<sup>41</sup> a soluble form of CD21 receptor. Control polymer without targeting peptides, P<sup>B</sup>, did not show any specific binding to either receptor-coated surface; while conjugates P<sup>B</sup>-A2-**B1**, P<sup>B</sup>-A3-**B1**, P<sup>B</sup>-A2-**P1**, and P<sup>B</sup>-A3-**P1** all showed specific binding toward both rsCR2.1-4- and sCD21-coated surfaces (Figure 7). P<sup>B</sup>-A3-**B1** showed higher binding than P<sup>B</sup>-A2-**B1** because of the spacer effect as discussed above, while P<sup>B</sup>-A2-**P1** and P<sup>B</sup>-A3-**P1** showed similar binding for the lacking of spacer effect.<sup>15</sup> The binding of P<sup>B</sup>-A3-**B1** was comparable to that of P<sup>B</sup>-A2-**P1** and P<sup>B</sup>-A3-**P1**, as the binding constant of **B1** ( $4.6 \times 10^6 \text{ M}^{-1}$ ) is only slightly higher than that of **P1** ( $2.9 \times 10^6 \text{ M}^{-1}$ ).<sup>15</sup> For unknown reasons, the binding of all four conjugates, P<sup>B</sup>-A2-**B1**, P<sup>B</sup>-A3-**B1**, P<sup>B</sup>-A2-**P1**, and P<sup>B</sup>-A3-**P1**, to the rsCR2.1-4-coated surface was higher than the binding to the sCD21-coated surface. Because **B1** was screened with rsCR2.1-4, the specific binding of HPMA copolymer-**B1** conjugates to sCD21 confirmed the successful identification of peptide ligands of CD21 receptor with our two-step fluorescence screening.

## Discussion

**Peptide Ligand Identification with the One-Bead One-Compound Combinatorial Method.** OBOC peptide libraries have been used to screen ligands for various targets, such as antibodies,<sup>23</sup> protease,<sup>42</sup> protein kinase, etc.<sup>24</sup> Successful identification of targeting peptides for lymphoma with OBOC has also been reported, with the target of surface idiotype of lymphoma cell lines,<sup>43</sup> and  $\alpha 4\beta 1$  integrin receptor in non-Hodgkin's lymphoma.<sup>44</sup> In this work, heptapeptide ligands of CD21 receptor, an alternative lymphoma target, were identified. Instead of focusing on validating the successful screening, this work further investigated the binding properties of one of the selected peptides, **B1**, after its conjugation with HPMA copolymer.

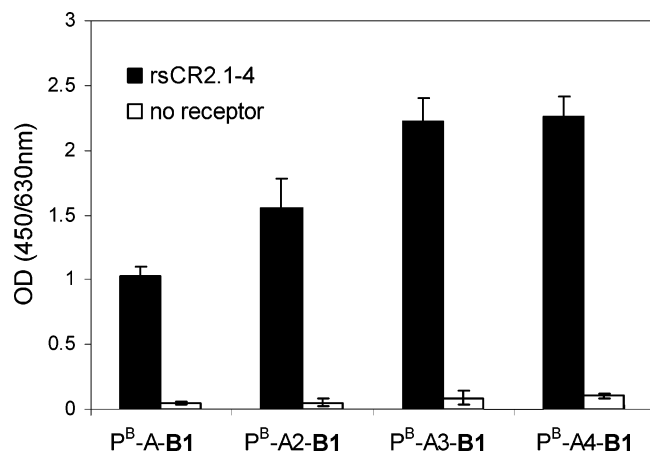
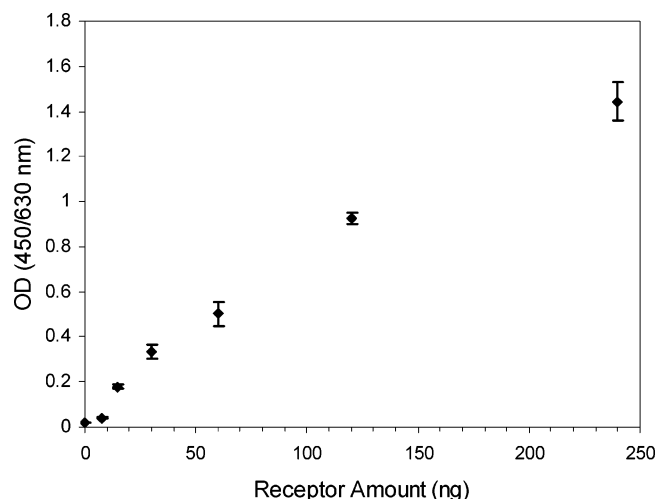
The one-bead one-compound combinatorial method has found its applications not only in peptide libraries, but also in other libraries with oligomers such as peptoids, oligocarbamates, oligoureas, etc., and with small molecules, as long as those libraries meet three requirements: first, well-established synthetic chemistry for library preparation; second, suitable screening method to distinguish desired products; and, third, appropriate decoding system for identification of selected compound.<sup>24</sup> The scope of OBOC was further broadened with the appearance of novel ideas in library preparation such as the one-bead two-



**Table 3.** Composition of HPMA Copolymer–Peptide Conjugates<sup>a</sup>

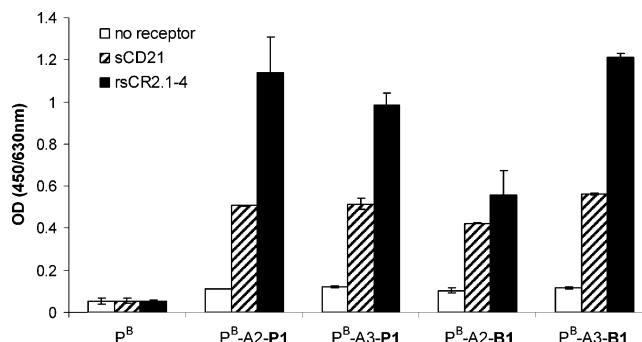
conjugates	structure	$M_w^b$ (kDa)	Pd <sup>c</sup>	peptide (mol %) <sup>d</sup>	peptide no./chain	biotin (mol %) <sup>e</sup>	biotin no./chain
P <sup>B</sup>	PHPMA–(PEG–biotin)	63.2	1.7	0	0	0.4	1.8
P <sup>B</sup> –A– <b>B1</b>	PHPMA–(A– <b>B1</b> )–(PEG–biotin)	42.1	1.4	2.1	5.2	0.34	1.0
P <sup>B</sup> –A2– <b>B1</b>	PHPMA–(A2– <b>B1</b> )–(PEG–biotin)	39.0	1.3	2.0	4.7	0.23	0.6
P <sup>B</sup> –A3– <b>B1</b>	PHPMA–(A3– <b>B1</b> )–(PEG–biotin)	38.7	1.3	2.2	4.9	0.45	1.2
P <sup>B</sup> –A4– <b>B1</b>	PHPMA–(A4– <b>B1</b> )–(PEG–biotin)	41.1	1.3	1.7	4.2	0.34	1.0
P <sup>B</sup> –A2– <b>P1</b>	PHPMA–(A2– <b>P1</b> )–(PEG–biotin)	55.6	1.5	1.1	4.3	0.36	1.4
P <sup>B</sup> –A3– <b>P1</b>	PHPMA–(A3– <b>P1</b> )–(PEG–biotin)	37.3	1.5	1.83	3.7	0.31	0.8

<sup>a</sup> P<sup>B</sup>: HPMA copolymer backbone labeled with a PEG<sub>3400</sub>–biotin graft. <sup>b</sup>  $M_w$ : weight-average molecular weight as determined with size-exclusion chromatography. <sup>c</sup> Pd: polydispersity, ratio of weight-average molecular weight over number-average molecular weight. <sup>d</sup> Determined with amino acid analysis. <sup>e</sup> Determined with EZ Biotin Quantitation Kit.

**Figure 5.** Surface binding results of HPMA copolymer–**B1** conjugates with different spacer lengths. Data are depicted as mean  $\pm$  standard deviation from duplicate measurements.**Figure 6.** The relationship between the binding of P<sup>B</sup>–A3–**B1** and amount of surface coating receptor. Data are depicted as mean  $\pm$  standard deviation from duplicate measurements.

compound library,<sup>45</sup> dimeric OBOC library,<sup>46</sup> and topologically segregated bilayer beads for OBOC,<sup>47</sup> new instrumentation like COPAS (Union Biometrica) for fluorescence screening,<sup>48</sup> and creative coding-decoding systems.<sup>49,50</sup>

There are several screening methods for OBOC libraries such as enzyme-linked colorimetric assay,<sup>23</sup> whole cell binding assay,<sup>44</sup> and autoradiography.<sup>51</sup> The enzyme-linked colorimetric assay usually requires a reporter protein for detection. Therefore, beads that specifically bind to the reporter protein have to be removed before screening. Otherwise, false positive beads might be selected. Fluorescence screening has no such problems, but its application has been largely limited by the autofluorescence

**Figure 7.** Comparison of surface binding results of HPMA copolymers containing peptides **B1** and **P1**. Data are depicted as mean  $\pm$  standard deviation from duplicate measurements.

of TentaGel. To overcome this limitation, instead of using traditional organic fluorophores, improved visualization has been achieved by labeling target molecules with quantum dots, because quantum dots provide higher quantum yield, and, more importantly, they exhibit narrower and symmetrical emission peaks.<sup>34,35</sup> Another approach is to remove autofluorescent beads before the binding assay with the aid of a fluorescence-activated COPAS sorter.<sup>48</sup> In this work, using a readily available organic fluorescein dye, this two-step fluorescence screening method proved to be successful for screening receptor bound beads. In addition, the discovery of the different fluorescence appearance of autofluorescent beads (transparent) and beads bound with fluorescently labeled receptor (opaque) provided a convenient method to expedite the fluorescence screening process. The different fluorescence appearance of selected beads in the first step also demonstrated different spatial fluorescence distribution as visualized with surface plotting (Figure 2C and F). Hypothetically, the different fluorescence appearance is the simple reflection of two different fluorescence mechanisms.

**Screening Results with OBOC.** Four different heptapeptide ligands of CD21 receptor were identified with the OBOC combinatorial method (Table 1). Previously, five different pentadecapeptide ligands were identified with phage display<sup>15</sup> (Table 2). As determined with a fluorescence quenching assay, the binding constants of peptide ligands selected with both methods were within the same range: with phage display, **P1**,  $2.9 \times 10^6 \text{ M}^{-1}$ ; **P2**,  $4.7 \times 10^6 \text{ M}^{-1}$ ; **P3**,  $2.2 \times 10^6 \text{ M}^{-1}$ , and with OBOC, **B1**,  $4.6 \times 10^6 \text{ M}^{-1}$ ; **B2**,  $1.0 \times 10^6 \text{ M}^{-1}$ ; **B3**,  $2.1 \times 10^6 \text{ M}^{-1}$ . Pentadecapeptide ligands did not demonstrate a much higher binding affinity than heptapeptides, probably because larger peptides have to overcome an extra entropy loss as compared to smaller peptides in their binding processes. All pentadecapeptide ligands showed a similar but much larger quenching ratio of  $\sim 70\%$ , while heptapeptide ligands only quenched 20–50% fluorescence. This probably suggests that larger peptide ligands, pentadecapeptides, induced a larger

conformational change of the receptor upon binding with ligand, most probably because their binding sites covered a larger area than the heptapeptide binding area. It is interesting to note that the peptide (**B1**) possessed both the highest binding constant ( $4.6 \times 10^6 \text{ M}^{-1}$ ) among the selected heptapeptides and the highest quenching ratio ( $\sim 50\%$ ). In contrast, the peptide (**B2**) having the lowest binding constant ( $1.0 \times 10^6 \text{ M}^{-1}$ ) also showed the lowest quenching ratio ( $\sim 20\%$ ), an indication of the possible relationship between the binding affinity of heptapeptides and quenching ratio.

The five pentadecapeptides, selected by phage display,<sup>15</sup> did not demonstrate much homology. However, three out of four OBOC selected heptapeptides, YILHRN, LVLLTRE, and IVFLLVQ, possessed some shared features: the first four amino acids at the N-terminus were mainly hydrophobic residues, leucine, isoleucine, and valine. By comparing the peptide sequences from OBOC with those from phage display, it was found the hydrophobic sections of peptides **B1**, **B2**, and **B3** are similar to segment LFLLV of peptide RLAYWCFSGL**LFLVC**, which was selected from phage display (similar residues are indicated in italic boldface type).<sup>15</sup> Such a resemblance is a significant indication of a peptide binding site, because in peptide RLAYWCFSGL**LFLVC**, LFLLV resides within two cysteines, which can form a cyclic structure, and such a structure is usually critical in binding.<sup>52</sup> Additionally, it was also found that peptide **B2** (PTLDPLP) has plausible similarity to peptide **PNLDFSPTCSFRFGC** selected from phage display.

**Spacer Effect on Binding of HPMA Copolymer–Peptide Conjugates.** There is evidence that the accessibility of a peptide can be influenced by conjugation with a polymer: the conjugation of a decapeptide (PYWKWQYKYD) with PEG 20 000 resulted in complete loss of reactivity, while its conjugation with PEG 5000 maintained its activity.<sup>40</sup> This was confirmed by the spacer effect in this work: the binding of HPMA copolymer–**B1** conjugates increased significantly with the increase of spacer length from A (8-amino-3,6-dioxaoctanoic acid) to A3 (trimer of A) (Figure 5). However, in our previous work, HPMA copolymer–**P1** conjugates,  $\text{P}^{\text{B}}\text{--GG--P1}$  and  $\text{P}^{\text{B}}\text{--A2--P1}$ , demonstrated similar binding to the rsCR2.1–4-coated surface, although spacer A2 (8-amino-3,6-dioxaoctanoyl-8-amino-3,6-dioxaoctanoic acid) in  $\text{P}^{\text{B}}\text{--A2--P1}$  is 4 times as long as the GG (glycylglycine) spacer in  $\text{P}^{\text{B}}\text{--GG--P1}$ ,<sup>15</sup> suggesting that the length of the spacer has little effect on the binding of HPMA copolymer–**P1** conjugates. Therefore, the spacer length showed different influences on the accessibility and the binding properties of peptides **B1** and **P1** in their HPMA copolymer conjugates. Hypothetically, this difference is ascribed to their different physical properties such as size and hydrophobicity/hydrophilicity of peptides. Pentadecapeptide **P1** (RMWPSSTVNL-SAGRR) is twice as long as heptapeptide **B1** (YILHRN), and thus has a better chance to expose itself. In addition, HPMA copolymer–**B1** conjugates may undergo a conformational change due to the amphipathic composition of **B1**, which may also contribute to the accessibility of **B1**.

**Structural Factors Influencing the Biorecognizability of HPMA Copolymer–Peptide Conjugates.** Undoubtedly, the biorecognizability of polymer–peptide conjugates is largely dictated by the intrinsic binding affinity between peptide ligands and its target molecules. Meanwhile, structural factors such as multivalency for interaction,<sup>12,15</sup> peptide accessibility, and polymer conformation<sup>53</sup> may also have a significant influence on the biorecognizability. The importance of multivalent interaction was clearly demonstrated in the binding studies of HPMA copolymer–**P1** conjugates containing various amounts

of **P1** peptide.<sup>15</sup> Being relatively small and chemically stable, peptides can be readily derivatized and incorporated into a polymers with multiple copies.<sup>54</sup> Thus, multivalency becomes one major advantage for the designing of polymer–peptide conjugates for targeted drug delivery. The accessibility of a peptide could be significantly weakened by the conjugation with polymers, consequently resulting in a decrease or total loss of binding activity.<sup>40</sup> It can be greatly improved with the introduction of spacers with sufficient length. The binding of HPMA copolymer–**B1** conjugates increased with the increase of spacer length from A to A3.

The conformation of HPMA copolymer may change drastically after being conjugated with multiple copies of peptide depending on the physical properties of the peptide and the content of peptide. Peptide YILHRN (**B1**) has an amphipathic structure with an N-terminal hydrophobic section (YILI) and a C-terminal hydrophilic section (HRN). It was found that the HPMA copolymer–**B1** conjugate has the tendency to self-associate with the increase of peptide content (to be published). In this work, HPMA copolymer–**B1** conjugates contain about 2% of peptide (approximately 5 peptides per polymer chain), and the degree of self-association was low. As  $\text{P}^{\text{B}}\text{--A3--B1}$  demonstrated comparable binding to  $\text{P}^{\text{B}}\text{--A3--P1}$ , the effect of self-association on the binding seemed to be limited. To evaluate the effect of self-association on the binding, various amounts of acrylic acid (10%, 20%, and 30%) were copolymerized with HPMA to disrupt the self-association process as a result of electrostatic expulsion. However, this effort was fruitless as the surface binding of HPMA copolymer–**B1** conjugates containing acrylic acid was totally abolished, indicating that acrylic acid interfered with the binding process.

**One-Bead One-Compound Peptide Library versus Phage Display Peptide Library.** Peptide ligands of CD21 receptor have been identified with OBOC, and, previously, with phage display.<sup>15</sup> Phage display is a biological combinatorial method: by engineering the DNA structure of phage, a phage peptide library is constructed, so that millions of different peptides are displayed on the phage capsid and are accessible for interaction with target proteins.<sup>29</sup> OBOC is a chemical combinatorial method: with the procedure of “split and mix”, an oligopeptide library could be constructed on the solid support such that each bead contains only one single peptide followed by on-resin immunological assays, which enable the identification of peptide ligands of receptor.<sup>24</sup> Both the OBOC method and phage display have been extensively used for selection and identification of oligopeptide ligands for tumor targeting.<sup>14</sup>

There are reports that peptide ligands with similar sequences were identified with both phage display and OBOC.<sup>55,56</sup> However, a full understanding of the advantages and the disadvantages of both phage display library and OBOC library is helpful for choosing appropriate combinatorial techniques for a specific screening purpose. With phage display, molecules of different sizes from oligopeptides to proteins can be displayed on phage coat protein. Phage display can also be conveniently used for identification of ligands for tumor tissue in vivo<sup>57</sup> and even with patient body.<sup>58</sup> The advantage of using OBOC to prepare the peptide library lies in its extraordinary control on the building blocks of the peptide library. The peptide sequence could be modified with D-amino acids or other unnatural amino acids to introduce desired properties. With the intercalation of structural determinants, the peptide structure on resin could be predefined: cyclic structure formation with disulfide bonds of two cysteines<sup>44</sup> and with side chains of lysine and glutamine,<sup>25</sup> and turn structure formation with proline.<sup>44</sup>



## Conclusions

With a two-step fluorescence screening process, the limitation caused by autofluorescence of TentaGel was avoided, and four heptapeptide ligands of CD21 receptor were successfully identified with the one-bead one-compound combinatorial method. The dissociation constants of all peptides except **B4** were determined with a fluorescence quenching assay to be within the micromolar range. HPMA copolymer conjugated with selected peptide, **B1**, demonstrated specific binding toward CD21 receptor. The binding between HPMA copolymer–**B1** conjugate and CD21 receptor was found to be dependent on the length of spacer between peptide and polymer backbone: spacers with sufficient length (A3 and A4) were able to significantly enhance the binding. With the proper spacer, HPMA copolymer equipped with selected heptapeptides seems to be a promising targeted anticancer drug carrier for chemotherapy of lymphoma. Combined with binding studies of HPMA copolymer containing targeting peptide derived from phage display,<sup>15</sup> this work should be informative for designing and optimizing other polymeric drug carriers containing targeting peptide in terms of structural factors such as peptide multivalency, peptide accessibility, and polymer conformation.

**Acknowledgment.** This work was supported in part by NIH grants CA88047 and CA51578 from the National Cancer Institute.

## References and Notes

- Kopeček, J. Soluble biomedical polymers. *Polim. Med.* **1977**, *7*, 191–221.
- Kopeček, J.; Kopečková, P.; Minko, T.; Lu, Z. HPMA copolymer-anticancer drug conjugates: design, activity, and mechanism of action. *Eur. J. Pharm. Biopharm.* **2000**, *50*, 61–81.
- Dreher, M. R.; Liu, W.; Michelich, C. R.; Dewhirst, M. W.; Yuan, F.; Chilkoti, A. Tumor vascular permeability, accumulation, and penetration of macromolecular drug carriers. *J. Natl. Cancer Inst.* **2006**, *98*, 335–44.
- Maeda, H.; Seymour, L. W.; Miyamoto, Y. Conjugates of anticancer agents and polymers: advantages of macromolecular therapeutics in vivo. *Bioconjugate Chem.* **1992**, *3*, 351–62.
- Shiah, J. G.; Dvořák, M.; Kopečková, P.; Sun, Y.; Peterson, C. M.; Kopeček, J. Biodistribution and antitumor efficacy of long-circulating *N*-(2-hydroxypropyl)methacrylamide copolymer-doxorubicin conjugates in nude mice. *Eur. J. Cancer* **2001**, *37*, 131–9.
- Rathi, R. C.; Kopečková, P.; Říhová, B.; Kopeček, J. *N*-(2-Hydroxypropyl)methacrylamide copolymers containing pendent saccharide moieties. Synthesis and bioadhesive properties. *J. Polym. Sci., Part A: Polym. Chem.* **1991**, *29*, 1895–991.
- Wróblewski, S.; Berenson, M.; Kopečková, P.; Kopeček, J. Potential of lectin-*N*-(2-hydroxypropyl)methacrylamide copolymer-drug conjugates for the treatment of pre-cancerous conditions. *J. Controlled Release* **2001**, *74*, 283–93.
- Omelyanenko, V.; Kopečková, P.; Gentry, C.; Shiah, J. G.; Kopeček, J. HPMA copolymer-anticancer drug-OV-TL16 antibody conjugates. 1. Influence of the method of synthesis on the binding affinity to OVCAR-3 ovarian carcinoma cells in vitro. *J. Drug Targeting* **1996**, *3*, 357–73.
- Shiah, J. G.; Sun, Y.; Kopečková, P.; Peterson, C. M.; Straight, R. C.; Kopeček, J. Combination chemotherapy and photodynamic therapy of targetable *N*-(2-hydroxypropyl)methacrylamide copolymer-doxorubicin/ mesochlorin e(6)-OV-TL 16 antibody immunoconjugates. *J. Controlled Release* **2001**, *74*, 249–53.
- Lu, Z. R.; Kopečková, P.; Kopeček, J. Polymerizable Fab' antibody fragments for targeting of anticancer drugs. *Nat. Biotechnol.* **1999**, *17*, 1101–4.
- Lu, Z. R.; Shiah, J. G.; Kopečková, P.; Kopeček, J. Polymerizable Fab' antibody fragment targeted photodynamic cancer therapy in nude mice. *S.T.P. Pharma Sci.* **2003**, *13*, 69–75.
- Tang, A.; Kopečková, P.; Kopeček, J. Binding and cytotoxicity of HPMA copolymer conjugates to lymphocytes mediated by receptor-binding epitopes. *Pharm. Res.* **2003**, *20*, 360–7.
- Line, B. R.; Mitra, A.; Nan, A.; Ghandehari, H. Targeting tumor angiogenesis: comparison of peptide and polymer-peptide conjugates. *J. Nucl. Med.* **2005**, *46*, 1552–60.
- Aina, O. H.; Sroka, T. C.; Chen, M. L.; Lam, K. S. Therapeutic cancer targeting peptides. *Biopolymers* **2002**, *66*, 184–99.
- Ding, H.; Proding, W. M.; Kopeček, J. Identification of CD21-binding peptides with phage display and investigation of binding properties of HPMA copolymer-peptide conjugates. *Bioconjugate Chem.* **2006**, *17*, 514–23.
- Press, O. W.; Leonard, J. P.; Coiffier, B.; Levy, R.; Timmerman, J. Immunotherapy of Non-Hodgkin's lymphomas. *Hematology (Am. Soc. Hematol. Educ. Program)* **2001**, 221–40.
- Proding, W. M. Complement receptor type two (CR2, CR21): a target for influencing the humoral immune response and antigen-trapping. *Immunol. Res.* **1999**, *20*, 187–94.
- Rask, R.; Rasmussen, J. M.; Hansen, H. V.; Bysted, P.; Svehaug, S. E. Complement C3dg/Epstein-Barr virus receptor density on human B-lymphocytes estimated by immunoenzymatic assay and immunocytochemistry. *J. Clin. Lab. Immunol.* **1988**, *25*, 153–6.
- Tang, A.; Kopeček, J. Presentation of epitopes on genetically engineered peptides and selection of lymphoma-targeting moieties based on epitope biorecognition. *Biomacromolecules* **2002**, *3*, 421–31.
- Hess, M. W.; Schwendinger, M. G.; Eskelinen, E. L.; Pfaller, K.; Pavelka, M.; Dierich, M. P.; Proding, W. M. Tracing uptake of C3dg-conjugated antigen into B cells via complement receptor type 2 (CR2, CD21). *Blood* **2000**, *95*, 2617–23.
- Proding, W. M.; Schoch, J.; Schwendinger, M. G.; Hellwege, J.; Parson, W.; Zipfel, P. F.; Dierich, M. P. Expression in insect cells of the functional domain of CD21 (complement receptor type two) as a truncated soluble molecule using a baculovirus vector. *Immunopharmacology* **1997**, *38*, 141–8.
- Liu, R.; Enstrom, A. M.; Lam, K. S. Combinatorial peptide library methods for immunobiology research. *Exp. Hematol.* **2003**, *31*, 11–30.
- Lam, K. S.; Salmon, S. E.; Hersh, E. M.; Hruby, V. J.; Kazmierski, W. M.; Knapp, R. J. A new type of synthetic peptide library for identifying ligand-binding activity. *Nature* **1991**, *354*, 82–4.
- Lam, K. S.; Lebl, M.; Krchnak, V. The “one-bead-one-compound” combinatorial library method. *Chem. Rev.* **1997**, *97*, 411–48.
- Lam, K. S.; Lehman, A. L.; Song, A.; Doan, N.; Enstrom, A. M.; Maxwell, J.; Liu, R. Synthesis and screening of “one-bead one-compound” combinatorial peptide libraries. *Methods Enzymol.* **2003**, *369*, 298–322.
- Frank, R. The SPOT-synthesis technique. Synthetic peptide arrays on membrane supports—principles and applications. *J. Immunol. Methods* **2002**, *267*, 13–26.
- Frank, R.; Overwin, H. SPOT synthesis. Epitope analysis with arrays of synthetic peptides prepared on cellulose membranes. *Methods Mol. Biol.* **1996**, *66*, 149–69.
- Smith, G. P. Filamentous fusion phage: novel expression vectors that display cloned antigens on the virion surface. *Science* **1985**, *228*, 1315–7.
- Smith, G. P.; Petrenko, V. A. Phage display. *Chem. Rev.* **1997**, *97*, 391–410.
- Stahl, S.; Uhlen, M. Bacterial surface display: trends and progress. *Trends Biotechnol.* **1997**, *15*, 185–92.
- Westerlund-Wikstrom, B. Peptide display on bacterial flagella: principles and applications. *Int. J. Med. Microbiol.* **2000**, *290*, 223–30.
- Furka, A. S.; Asgedom, M.; Dibo, G. Cornucopia of peptides by synthesis. *Highlights Mod. Biochem., Proc. Int. Congr. Biochem.*, *14th* **1988**, *5*, 47–47.
- Furka, A. S.; Asgedom, M.; Dibo, G. More peptide by less labour. Poster presented at Xth International Symposium on Medicinal Chemistry, Budapest, 1988.
- Olivos, H. J.; Bachhawat-Sikder, K.; Kodadek, T. Quantum dots as a visual aid for screening bead-bound combinatorial libraries. *ChemBioChem* **2003**, *4*, 1242–5.
- Garske, A. L.; Denu, J. M. SIRT1 top 40 hits: use of one-bead, one-compound acetyl-peptide libraries and quantum dots to probe deacetylase specificity. *Biochemistry* **2006**, *45*, 94–101.
- Lin, M.; Nielsen, K. Binding of the Brucella abortus lipopolysaccharide O-chain fragment to a monoclonal antibody. Quantitative analysis by fluorescence quenching and polarization. *J. Biol. Chem.* **1997**, *272*, 2821–7.
- Prota, A. E.; Sage, D. R.; Stehle, T.; Fingerroth, J. D. The crystal structure of human CD21: Implications for Epstein-Barr virus and C3d binding. *Proc. Natl. Acad. Sci. U.S.A.* **2002**, *99*, 10641–6.

- (38) Szakonyi, G.; Guthridge, J. M.; Li, D.; Young, K.; Holers, V. M.; Chen, X. S. Structure of complement receptor 2 in complex with its C3d ligand. *Science* **2001**, *292*, 1725–8.
- (39) Miller, R. T.; Kubier, P. Blocking of endogenous avidin-binding activity in immunohistochemistry: The use of egg whites. *Appl. Immunohistochem.* **1997**, *5*, 63–6.
- (40) Kopecky, E. M.; Greinstetter, S.; Pabinger, I.; Buchacher, A.; Romisch, J.; Jungbauer, A. Effect of oriented or random PEGylation on bioactivity of a factor VIII inhibitor blocking peptide. *Biotechnol. Bioeng.* **2006**, *93*, 647–55.
- (41) Fremeaux-Bacchi, V.; Kolb, J. P.; Rakotobe, S.; Kazatchkine, M. D.; Fischer, E. M. Functional properties of soluble CD21. *Immunopharmacology* **1999**, *42*, 31–7.
- (42) Meldal, M.; Svendsen, I.; Breddam, K.; Auzanneau, F. I. Portion-mixing peptide libraries of quenched fluorogenic substrates for complete subsite mapping of endoprotease specificity. *Proc. Natl. Acad. Sci. U.S.A.* **1994**, *91*, 3314–8.
- (43) Lam, K. S.; Lou, Q.; Zhao, Z. G.; Smith, J.; Chen, M. L.; Pleshko, E.; Salmon, S. E. Idiotypic specific peptides bind to the surface immunoglobulins of two murine B-cell lymphoma lines, inducing signal transduction. *Biomed. Pept., Proteins Nucleic Acids* **1995**, *1*, 205–10.
- (44) Park, S. I.; Manat, R.; Vikstrom, B.; Amro, N.; Song, L.; Lam, K. S. The use of one-bead one-compound combinatorial library method to identify peptide ligands for  $\alpha 4\beta 1$  integrin receptor in non-Hodgkin's lymphoma. *Lett. Pept. Sci.* **2002**, *8*, 171–8.
- (45) Meldal, M. The one-bead two-compound assay for solid-phase screening of combinatorial libraries. *Biopolymers* **2002**, *66*, 93–100.
- (46) Aggarwal, S.; Harden, J. L.; Denmeade, S. R. Synthesis and screening of a random dimeric peptide library using the one-bead-one-dimer combinatorial approach. *Bioconjugate Chem.* **2006**, *17*, 335–40.
- (47) Wang, X.; Peng, L.; Liu, R.; Xu, B.; Lam, K. S. Applications of topologically segregated bilayer beads in “one-bead one-compound” combinatorial libraries. *J. Pept. Res.* **2005**, *65*, 130–8.
- (48) Kodadek, T.; Reddy, M. M.; Olivos, H. J.; Bachhawat-Sikder, K.; Alluri, P. G. Synthetic molecules as antibody replacements. *Acc. Chem. Res.* **2004**, *37*, 711–8.
- (49) Wang, X.; Peng, L.; Liu, R.; Gill, S. S.; Lam, K. S. Partial alloc-deprotection approach for ladder synthesis of “one-bead one-compound” combinatorial libraries. *J. Comb. Chem.* **2005**, *7*, 197–209.
- (50) Song, A.; Zhang, J.; Lebrilla, C. B.; Lam, K. S. A novel and rapid encoding method based on mass spectrometry for “one-bead-one-compound” small molecule combinatorial libraries. *J. Am. Chem. Soc.* **2003**, *125*, 6180–8.
- (51) Kassarian, A.; Schellenberger, V.; Turck, C. W. Screening of synthetic peptide libraries with radiolabeled acceptor molecules. *Pept. Res.* **1993**, *6*, 129–33.
- (52) Aina, O. H.; Marik, J.; Liu, R.; Lau, D. H.; Lam, K. S. Identification of novel targeting peptides for human ovarian cancer cells using “one-bead one-compound” combinatorial libraries. *Mol. Cancer Ther.* **2005**, *4*, 806–13.
- (53) Itoda, K.; Tamiya, E.; Yokoyama, K. Evaluation of the molecular recognition of peptide-conjugated polymer. *Anal. Sci.* **2003**, *19*, 185–7.
- (54) Sadler, K.; Zeng, W.; Jackson, D. C. Synthetic peptide epitope-based polymers: controlling size and determining the efficiency of epitope incorporation. *J. Pept. Res.* **2002**, *60*, 150–8.
- (55) Salmon, S. E.; Lam, K. S.; Lebl, M.; Kandola, A.; Khattri, P. S.; Wade, S.; Patek, M.; Kocis, P.; Krchnak, V.; Thorpe, D.; Felder, S. Discovery of biologically active peptides in random libraries: solution-phase testing after staged orthogonal release from resin beads. *Proc. Natl. Acad. Sci. U.S.A.* **1993**, *90*, 11708–12.
- (56) Healy, J. M.; Murayama, O.; Maeda, T.; Yoshino, K.; Sekiguchi, K.; Kikuchi, M. Peptide ligands for integrin  $\alpha v \beta 3$  selected from random phage display libraries. *Biochemistry* **1995**, *34*, 3948–55.
- (57) Kolonin, M.; Pasqualini, R.; Arap, W. Molecular addresses in blood vessels as targets for therapy. *Curr. Opin. Chem. Biol.* **2001**, *5*, 308–13.
- (58) Arap, W.; Kolonin, M. G.; Trepel, M.; Lahdenranta, J.; Cardo-Vila, M.; Giordano, R. J.; Mintz, P. J.; Ardel, P. U.; Yao, V. J.; Vidal, C. I.; Chen, L.; Flamm, A.; Valtanen, H.; Weavind, L. M.; Hicks, M. E.; Pollock, R. E.; Botz, G. H.; Bucana, C. D.; Koivunen, E.; Cahill, D.; Troncoso, P.; Baggerly, K. A.; Pentz, R. D.; Do, K. A.; Logothetis, C. J.; Pasqualini, R. Steps toward mapping the human vasculature by phage display. *Nat. Med.* **2002**, *8*, 121–7.

BM060508F